Multiaxial Fatigue Resistance in Thermoplastics and Correlation to Cyclic Behavior

S. Castagnet, Y. Nadot, A. Berrehili and J. C. Grandidier

Institut P', Département de Physique et Mécanique des Matériaux, ENSMA, 1 Avenue Clément Ader, BP 40109, 86961 Futuroscope cedex, France – sylvie.castagnet@lmpm.ensma.fr , yves.nadot@lmpm.ensma.fr

ABSTRACT. *In the first part, the multiaxial fatigue behavior of a high-density polyethylene (HDPE) was investigated at room temperature and constant frequency. As a consequence of the mode of failure, an end-of-life criterion for fatigue tests was discussed first, in order to define the number of cycles to failure. Based on force controlled fatigue tests under tension, compression and torsion at two stress ratio, a multiaxial fatigue criterion including the stress-ratio effect is proposed for the fatigue design of this polymer. This criterion is based on the maximum and mean values of the second invariant of the stress tensor. The second part focuses on the cyclic behavior components in order to highlight the issue of a stabilized mechanical state as an input for the fatigue criterion. Experiments and numerical simulations are presented.*

INTRODUCTION

The design of structural parts made of thermoplastics requires relevant constitutive laws and criteria over a wide range of solicitations, among which fatigue loading. In this field, many works have been reported about rubbers [1,2] and filled-thermoplastics, in particular about short glass fiber-reinforced thermoplastics [3,4]. In the later case, most studies dedicated to incremental approaches or criteria accounting for the anisotropy induced by fillers. Most of time, despite a usually complex behavior due to time-dependent mechanisms and thermo mechanical coupling, the thermoplastic matrix has been considered as being elastic.

Works in unfilled thermoplastics mostly focused on fatigue crack propagation, and its competition with plasticity. They were often based on tension-compression experiments and mainly performed to compare materials [5-7]. Fatigue tests have been mainly conducted in a uniaxial framework, under stress or strain controlled sinusoidal tension-tension or tension-compression waveforms. Only a few works were carried out in the range of high-cycle fatigue and biaxial loading [8,9] or flexural [10] loading mode. The influence of some microstructure parameters has been investigated [11-13]. On this topic, a lot of attention has been paid on ultra-high molecular weight polyethylene [11].

Multiaxial fatigue life estimation of engineering materials has been a challenging task for over past decades, but so far there have been only a few studies in un-filled and un_notched semi-crystalline thermoplastics. Only a few works have reported fatigue lifetime estimation in un-notched polyolefines [14,15]. However, an effective multiaxial fatigue criterion is needed for practical applications since most of the load-bearing components are used under multiaxial loading conditions.

The first aim of this paper is to propose a multiaxial endurance fatigue criterion for an un-cracked semi-crystalline polymer, after defining an end-of-life criterion in such samples failing by instability. The endurance fatigue behavior of a widely-used high-density polyethylene (HDPE) is addressed under tensile, compressive and torsion loadings, at different R-ratio (0, -∞ and -1) and constant frequency. In such materials exhibiting softening during cyclic loading, a suitable "stabilized" mechanical state must be defined and calculated as a fatigue criterion input. The phenomenon is well known in rubbers which are previously "accommodated" by cycling loading before fatigue design. In the same way, it can be needed to characterize and model a relevant "accommodated" state in thermoplastics, if existing. Few experimental and theoretical works were proposed about cyclic behavior [16-18], but most of time, a few cycles have been considered. Highlighting this issue is the second aim of this paper.

EXPERIMENTAL

Material

This study was conducted in a HDPE provided by Ineos in the form of 50 mm external diameter and 3.2 mm thick extruded pipes, allowing performing all multiaxial tests on the same shape and thus avoiding microstructure differences enhanced by the process in case of variable geometry. Samples were cut with a 70 mm gauge length l^0, machined with a very smooth curvature radius: the internal diameter was unchanged all along the tubular sample and the minimal thickness was 2.5 mm. For fatigue tests, tubular samples were mounted between two aluminum grips inside and outside the pipe.

Multiaxial fatigue tests

All multiaxial fatigue tests were performed at room temperature on a servo-hydraulic biaxial testing machine. Force controlled tests were conducted in tension, compression and torsion, using a triangular wave function in order to keep a constant stress-rate all along the test, for correlation purpose with the second part of the work. Tests have been conducted at a constant frequency selected to reduce the possibility of self-heating and thermal failure. Besides, fatigue tests were performed by placing the grips and sample within a purpose-designed temperature-controlled chamber (±0.5°C), where the same cooled air flux circulates inside and around the pipe. The initial ambient temperature was 18.8 ± 0.3°C (averaged from 30 tests).

The tension/compression and torsion stresses (σ_{zz} and $\tau = \sigma_{z\theta}$ respectively) and strains (ε_{zz} and $\varepsilon_{z\theta}$ respectively) were calculated in the minimal section of the pipe,

from the four mechanical data monitored during the experimental tests (i.e. the applied force, the torque, the piston displacement and the angular variation) in a thin-walled pipe assumption framework, i.e. at the median radius of the pipe wall. Since the diameter reduction could not be accessed during the test, only the longitudinal nominal stress in the minimal diameter section was considered. In the same way, applied stress-rates were nominal ones. Here, the von Mises stress (vM index) and the maximum Principal stress (P index) are discussed for evaluation of multiaxial loading. In case of tension loading, $\sigma_{zz} = \sigma_{vM} = \sigma_P$. In case of torsion loading, $\sigma_{vM} = \sqrt{3}\,\tau$ and $\sigma_P = \tau_{nom}$. Four temperature measurements were monitored at the same time, at the inner and outer surface of the pipe and in the ambient air inside and outside the pipe. The stress amplitude σ_a was defined as the difference between the maximum and the mean stresses. The stress ratio R (defined as the minimum stress divided by the maximum stress over the fatigue cycle) was 0 or -1. In the following, fatigue tests performed at R=0 or R=-∞ will be called "pulsating" tests in tension and compression respectively, and those carried out at R=-1 will be called "fully reversed" ones. The so-called "fully reversed tension loading at R=-1" is actually a tension/compression loading mode. In the following, the index $_a$, $_{max}$ and $_{mean}$ will always refer to the amplitude, maximum and mean value of the considered variable respectively.

RESULTS

Definition of an end-of-life criterion

The usual S-N curves obtained at 2Hz in pulsating or fully reversed tension (R=0; R=-1), pulsating compression (R=-∞) and pulsating or fully reversed torsion (R=0; R=-1) are shown in Figure 1. The maximum of the stress absolute value σ_{max} (tension or compression) or τ_{max} (torsion) is plotted vs. log (cycles to failure) or log N_m. Such S-N curves can be fitted by Equation (1) where β, A and c are parameters.

$$\sigma_a = \beta + \frac{A}{N_m{}^C} \tag{1}$$

In Figure 1, the number of cycles to failure N_m corresponds to the overcome of the maximum values assigned by the operator to the axial or angular displacement of the cylinder. It means that the sample is bound to undergo a large number of cycles after necking or buckling, before reaching the displacement limits of the servo-hydraulic machine. Thus, N_m is not intrinsic. Subsequently, a more objective end-of-life criterion must be defined before considering the fatigue tests results. To detect the onset of macroscopic instability, the evolution of the maximum, minimum and mean strains of the fatigue loops was tracked along the fatigue test. They are plotted against the number of cycles in Figure 2 (left), for a tensile fatigue test performed at R=0 and a maximum applied stress of 22.6 MPa. Each of the three strains follows a slowing-down regime, before reaching a stationary stage and finally exhibiting a drastic increase of the strain-rate. By analogy with the primary, secondary and tertiary stages usually distinguished in monotonic creep at constant nominal stress, the inflexion point on the mean strain vs.

number of cycles curve is associated with the onset of a softening process assumed here to be the macroscopic instability leading to failure. Thus, in addition to the final number of cycles N_m (recorded when reaching the hydraulic limits of the machine; 15330 cycles in Figure 2), two end-of-life criteria can be defined: N_i corresponds to the number of cycles at the inflexion point and thus at the onset of instability (N_i = 8800 cycles in Figure 2) while N_f refers to the maximum number of cycles at the end of the stationary stage before drastic localization of the macroscopic strain (N_f = 13500 cycles in Figure 2). N_f corresponds to a 2 % deviation of between the experimental strain value and the value extrapolated from the tangent curve at the inflexion point.

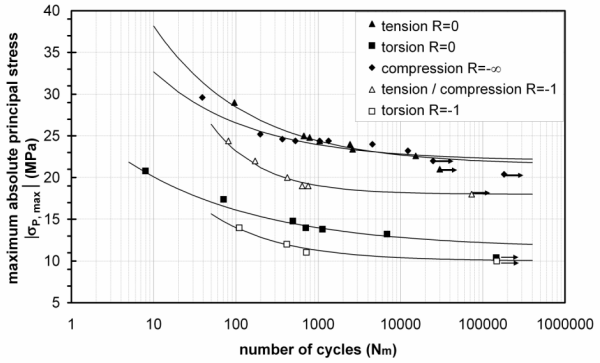

Figure 1. S-N curves in tension, torsion and compression at different R-ratio.

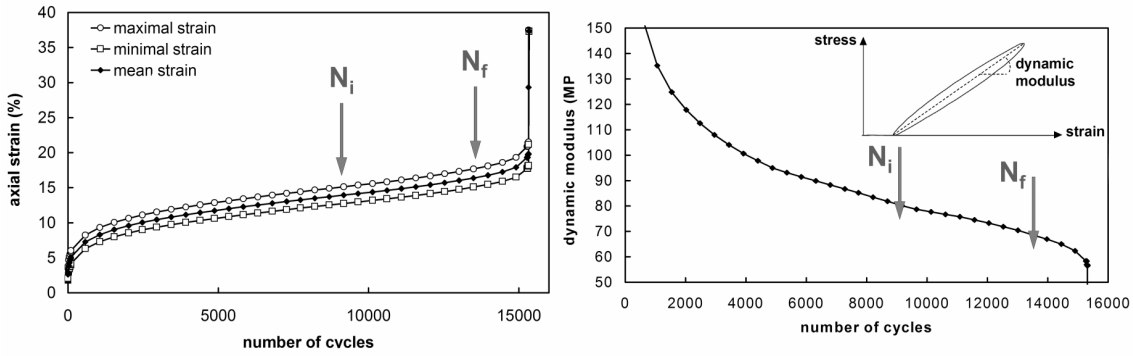

Figure 2. Evolution of (left) the maximum, minimum and mean strains, and (right) the dynamic modulus during a tensile fatigue test at R=0 (σ_{max}=22.6 MPa).

Figure 2 (right) represents the evolution of the dynamic modulus, defined as the slope of the straight line joining the initial point and the maximum stress/strain point of the fatigue loop. This modulus exhibits primary, stationary and tertiary stages with an inflexion point seated nearly at N_i. The decrease of dynamic modulus in the first thousands of cycles accounts for the viscoelastic contribution and the final drop of stiffness to the macroscopic strain localization. Tension, torsion and compression loadings at R=0, R=-1 or R=-∞, with an identical maximum von Mises stress of 24.4 MPa, were considered, showing that the proposed end-of-life criterion could be applied.

It must be mentioned that the way of defining the number-of-cycles-to-failure mainly affects the short lifetimes, whereas over 10^3 cycles, i.e. in the lifetime range focused in this paper, the three curves nearly overlap. In the following, S-N curves will be plotted as a function of the number of cycles N_i at the onset of instability, in the same way as initiation curves for cracked materials.

Multiaxial Fatigue Criterion

The same data as presented in Figure 1 are plotted again in Figure 3 as a function of N_i, for a principal stress analysis. Absolute values of the principal stress amplitude (σ_a in tension and compression or τ_a in torsion) (Figure 3-left) or the maximum principal stress (σ_{max} in tension and compression or τ_{max} in torsion) (Figure 3-right) are plotted vs. log (cycles to failure) or log N_i. Nor the amplitude neither the maximum value of the principal stress appears to be a satisfying equivalent stress to capture the multiaxial dependence of the fatigue behavior, if especially the shear stress is presented in the principal stress system.

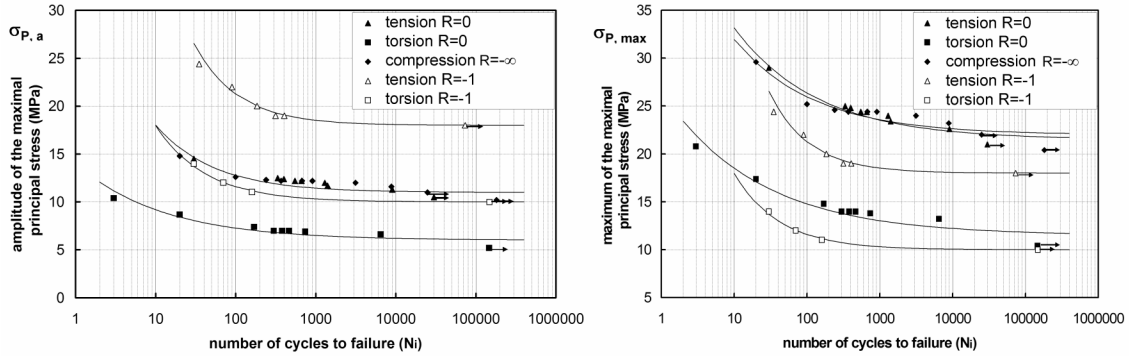

Figure 3. S-N_i curves from tension, torsion and compression tests at various R-ratio, plotted with the (left) amplitude and (right) maximum value of the principal stress.

It was observed that the von Mises equivalent stress, corresponding to the square-root of the second invariant of the stress tensor, was more suitable to describe the multiaxial fatigue behavior at a given R-ratio. Figure 4 (left) suggests a good relevance of the second invariant of the stress tensor J_2 to account for the fatigue life behavior of HDPE. Thus, the fatigue life behavior of this polymer strongly depends on shear processes. However, the maximum von Mises equivalent stress does not account for the R-ratio effect. By comparison with pulsating loading (R=0), the material submitted to a fully reversed loading (R=-1) undergoes a lower number of cycles to failure.

Neither the Crossland criterion nor the Sines one, also involving the second invariant J_2 in addition to the maximum $J_{1,max}$ and mean value $J_{1,mean}$ of the first invariant J_1 (hydrostatic stress) respectively, were relevant to capture both the different loading paths and the R-ratio (0, -∞ and -1). One possibility for that, proposed here, was

to complete the von Mises criterion with an additional term, still based on J_2, but on the mean value, as expressed by Equation (2):

$$\sigma_{eq} = \sqrt{J_{2\,max} + \alpha J_{2mean}} \leq \beta + \frac{A}{N_i^{\,C}} \qquad (2)$$

where α, β, A and c are parameters. The previously introduced fitting of the Wöhler curve appears on the right side of the criterion, as parametered by β, A and c. The relationship between this new equivalent stress and the number of cycles to failure N_i is illustrated in Figure 4 (right) for the five different loading situations tested here.

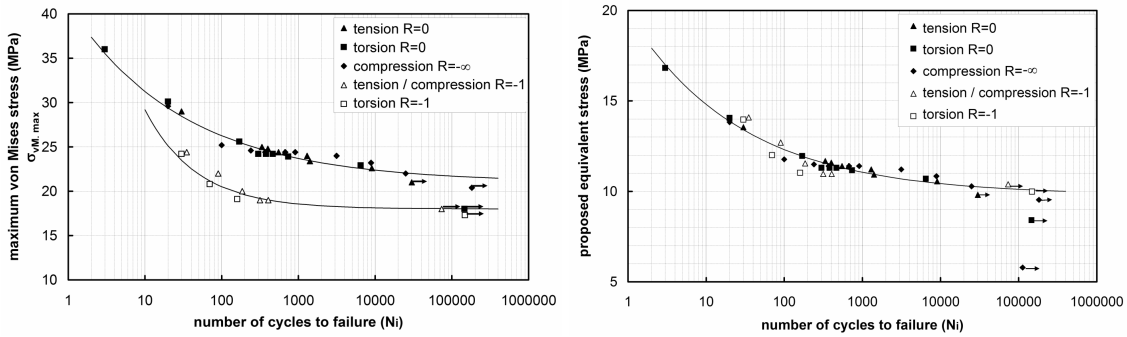

Figure 4. S-N_i curves obtained from fatigue tests in tension, torsion and compression at various R-ratio, plotted along the vertical axis with the (left) von Mises equivalent stress and (b) the proposed equivalent stress.

This criterion needs two Wöhler curves for the identification: β, A and c can be fitted from a first Wöhler curve in fully reversed tension at R=-1 for which J_{2mean} is zero (parameter β equals 10.4 here and corresponds to the fatigue strength at $N=10^5$ cycles); α can be identified further from a second Wöhler curve in pulsating tension at R=0 (the α value is -1.38). Then, the fatigue life behavior in pulsating compression at R=-∞, torsion at R=0 and R=-1 can be predicted. It is remarkable that this criterion, identified from tension at R=0 and R=-1 only, is able to capture pure torsion fatigue at both load ratio. Therefore, a good description of more complex stress states could be expected but it should be obviously validated from more experiments. To account for the R-ratio effect, another possibility could be to evaluate the mean stress sensitivity parameter by using the results at R = -1 and R = 0 for both loadings.

Analysis of the cyclic behavior components

This part aims at discussing the existence and definition of a stabilized state. Indeed, predicting the fatigue life of complex structures both requires a suitable criterion and a realistic mapping of stress and strain fields onto apply the fatigue life criterion. A simulation of the first cycle loading may not be relevant in polymers, due to viscosity. Thus, the coupled viscoelastic, viscoplastic and damage contributions to the cyclic behavior must be understood.

One-dimensional cyclic tensile tests have been considered first. The evolution of moduli, strains (strain at the end of loading, strain after unloading and mean strain of the

cycle) and hysteresis area was followed during the first thousand cycles. As illustrated in Figure 5, the cyclic response reaches an « accommodated » state, with a stabilization of the hysteresis area. The mean strain keeps increasing following kinetics much slower than the cycling period. Two distinct time scales can be pointed out, respectively associated with short relaxation times close to the loading period, and longer relaxation times enhancing creep under the mean stress.

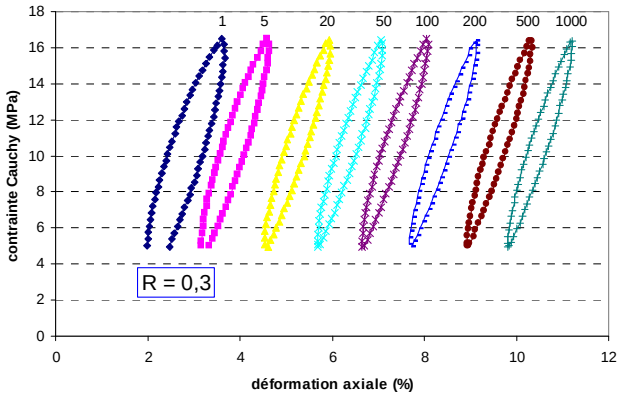

Figure 5: Evolution of hysteresis area during cyclic tensile loading (triangular loading; R=0.3; maximal stress 16.5 MPa).

Several loading factors, like stress rate, load ratio, mean stress have been investigated. Some tensile loading tests have been followed by relaxation stages to evaluate recovery and track the viscoelastic contribution. Viscoelasticity has been found out to greatly contribute to the creep effect under mean stress. Viscoplastic and/or damage contributions also increase during cycling. This first series of experimental results has been compared to numerical simulations performed in the Finite Elements Code Abaqus® using a viscoelastic constitutive law, in an isothermal framework. Work is in progress to build a suitable constitutive law accounting for the time scale separation depicted above.

The second part of the study involves widened fatigue conditions in terms of multiaxial loadings, load ratio and frequency. The evolution of mean strain, modulus and hysteresis area has been analyzed in the same way as depicted in the first part. In particular, the role of mean stress, frequency and loading path has been emphasized.

As an example, tests performed at R=0 in tension (maximum principal stress 24.4 MPa; 2Hz) were interrupted before failure and followed by a several hours strain recovery. It was shown that, when cycling is stopped below N_i, the mean strain induced by cycling appears fully recovered while an increasing plastic contribution is observed after a number of cycles exceeding N_i. The plastic component of the strain keeps moderate but accumulation can be characterized. These results suggest that the fatigue behavior of this material up to the onset of instability is widely influenced by a viscoelastic contribution. As viscoelasticity and damage are known to be strongly correlated in these materials [19], mechanisms leading to fatigue failure need careful analysis.

CONCLUSION

Force-controlled multiaxial fatigue tests (tension, torsion, compression) have been performed in thin-walled tubular specimens of HDPE, with a constant frequency, a triangular waveform and different R-ratio (0, -∞ and -1). Self-heating has been minimized and results have been interpreted in an isothermal framework.

Considering the failure mode, an end-of-life criterion has been defined first, based on the onset of softening detected on the time evolution of the fatigue loop mean strain. Based on this end-of-life criterion, S-N curves could be drawn up. A fatigue criterion, expressed from the maximum and mean values of the second-invariant of the stress tensor, has been proposed to account for the endurance lifetime sensitivity to the loading path and the R-ratio (0, -1 and -∞). This stress-based criterion was validated for the restrictive framework of force-controlled fatigue tests, over similar mean stress conditions between tension and torsion. The application to other types of loadings was not discussed here. More general loading conditions should be considered before generalization.

Designing parts made of such materials from a fatigue-criterion approach needs a stabilized mechanical state. A great amount of the cyclic strain has been demonstrated to be viscoelastic and thus recoverable after cycling interruption. This must be taken into account in the constitutive law aimed at simulating the stabilized state. Work is in progress to include other components.

REFERENCES

1. Mars WV, Fatemi A (2002) *Int. J. Fat.* **24**, 949-961.
2. Verron E, Andriyana A (2008) *J Mech. Phys. Solids*, **58**, 417-443.
3. Sonsino CM, Moosbrugger E (2008) *Int. J. Fat.* **30**, 1279-1288.
4. Nouri H, Meraghni F, Lory P (2009) *Int. J. Fat.* **31**, 934-942.
5. Pruitt L, Bailay L (1998) *Polymers* **39** 1545.
6. Parson M, Stepanov EV, Hiltner A, Baer E (2000) *J. Mat. Science*, **35**, 2659.
7. Chen X, Hui S (2005) *Polym. Test.*, **24**, 829-833.
8. Leevers PS, Culver LE, Radon JC (1979) *Eng. Fract. Mech*. 11, 487-498.
9. Xia Z, Hu Y, Ellyin F (2003) *Polym. Eng. Sci.* **43**, 734.
10. Ramsteiner F, T. Armbrust, Polym. Test. 20 (2001) 321-327.
11. Pruitt LA (2005) *Biomaterials* **26**, 905-915.
12. Sauer JA, Hara M (1990) *Adv. Polym. Sci.* **91-92**, 69-118.
13. Runt J, Gallagher KP (1991) *J. Mat. Sci.* **26**, 792-798.
14 Kultural SE, Eryurek IB (2007) *Materials & Design* **28**, 816-823.
15. Janssen RPM, Govaert LE, Meijer HEH (2008) *Macromol*. **41**, 2531-2540.
16. Chen, X, Hui S (2005) *Polymer Testing* **24**, 829-833.
17. Bergström JS, Kurtz SM et al. (2002) *Biomaterials* **23**, 2329-2343.
18. Drozdov AD, Christensen JC (2007) *Polymer* **48**, 3003-3012.
19. Castagnet S, Girault S, Gacougnolle JL, Dang P (2000) *Polymer* **41**, 7523–7530.